Journal of Power and Energy Engineering, 2023, 11, 1-24
https://www.scirp.org/journal/jpee
ISSN Online: 2327-5901
ISSN Print: 2327-588X

Design and Development of Wind-Solar Hybrid Power System with Compressed Air Energy Storage for Voltage and Frequency Regulations

Banet Masenga[1*#], Jean Byiringiro[1*], Charles Kagiri[1*], Edwell Tafara[2*], Daniel Ngoma[3*], Gnoumou Aristid[4*]

[1]Mechatronic Engineering Department, Dedan Kimathi University of Technology, Nyeri, Kenya
[2]Electrical Engineering Department, Dedan Kimathi University of Technology, Nyeri, Kenya
[3]Mechanical Engineering Department, Arusha Technical College, Arusha, Tanzania
[4]Industrial Engineering Department, Université de Lisala, Bukavu, Democratic Republic of Congo
Email: #masengabanet@gmail.com

How to cite this paper: Masenga, B., Byiringiro, J., Kagiri, C., Tafara, E., Ngoma, D. and Aristid, G. (2023) Design and Development of Wind-Solar Hybrid Power System with Compressed Air Energy Storage for Voltage and Frequency Regulations. *Journal of Power and Energy Engineering*, **11**, 1-24.
https://doi.org/10.4236/jpee.2023.112001

Received: January 30, 2023
Accepted: February 24, 2023
Published: February 27, 2023

Abstract

The intermittent nature of wind and solar photovoltaic energy systems leads to the fluctuation of power generated due to the fact that the power output is highly dependent upon local weather conditions, which results to the load shading issue that led to the voltage and frequency instability. In additional to that, the high proportions of erratic renewable energy sources can lead to erratic frequency changes which affect the grid stability. In order to reduce this effect, the energy storage system is commonly used in most wind-solar energy systems to balance the voltage and frequency instability during load variations. One of the innovative energy storage systems is the compressed air energy storage system (CAES) for wind and solar hybrid energy system and this technology is the key focus in this research study. The aim of this research was to examine the system configuration of the CAES system through modelling and experimental approach with PID controller design for regulating the voltage and frequency under different load conditions. The essential elements and the entire system have been presented in this work as thorough modelling in the MATLAB/Simulink environment for different load conditions. The developed model was tested through an experimental workbench using the developed prototype of the compressed air storage in the Siemens Lab at DeKUT and explored the consequence of the working parameters on the system proficiency and the model accuracy. The performance

*These Authors contributed equally to this work.
#Corresponding author.

of the system for the developed prototype of CAES system was validated using results from an experimental workbench with MATLAB/Simulink R2022b simulation. The modeling and experimental results, shows that the frequency fluctuation and voltage drop of the developed CAES system during load variations was governed by the I/P converter using a PID_Compact controller programed in the TIA Portal V17 software and downloaded into PLC S7 1200. Based on these results, the model can be applied as a basis for the performance assessment of the compressed air energy storage system so as to be included in current technology of wind and solar hybrid energy systems.

Keywords

Voltage, Frequency, Compressed Air Energy Storage, Load Variations, PID Control, I/P Converter Valve

1. Introduction

In many states, shifting power utilities have attracted attention toward more energy-efficient and renewable power sources. Solar Photovoltaic energy systems are becoming more common among all renewable energy sources [1]. However, a proper control algorithm is vital to monitor the Solar Photovoltaic energy system for grid or residential applications since the nature of solar irradiance and load changes rapidly [1] and this affects the amount of power produced on the system. Most rural areas and small remote islands especially in Africa do not benefit from power supply from the main grid [2] because of the less transmission lines. Currently, energy demand for these locations is mainly supplied through diesel engine generation systems [3] and also some isolated solar and wind mini grid. However, the applications of diesel generator systems have becoming a problem due to rising environmental issues and high running costs [4] and hence not recommended for many utility companies. Due to this effect, a hybrid power supply system could be an alternative solution to supply electricity to most rural and remote off-grid areas. A typical hybrid power system may contain several renewable energy sources such as wind, solar and other renewable energy sources [5] that can be integrated to increase power supply. Based on the availability of energy resources, a proper combination of renewable energy sources can be exploited to form a hybrid power system [6] that is suitable to a local area in an off-grid location. Wind power systems are one of the energy technologies to utilize, and when used appropriately, they may satisfy the rising need for power in inaccessible locations where the wind is freely available [2]. However, there are various problems accompanied in designing these power systems [2] and some of them have been highlighted in this research study which include voltage and frequency control and monitor [7]. In addition to that, a more detailed study on power quality and synchronization among different components and cost-effectiveness of the power systems are areas that need more research and development [8].

In energy system comparison, wind turbines need regular maintenance and are susceptible to damage in strong winds [9] and hence not suitable as isolated energy supply systems. On the other hand, photovoltaic solar power systems are dependent on the local weather conditions, seasons of the year, and geographic location of the place. Due to potential system issues including voltage instability and substantial frequency variation, the necessity for energy storage for power stability must be taken into account [10].

Based on the two energy technologies, it has been noted that a hybrid energy system especially from renewables can significantly decrease the total life cycle cost of power supplies in many situations while simultaneously providing an extra and reliable supply of electric power through synchronizing the energy sources [11] and this idea have been implemented in this research study.

The electrical energy from wind and solar energy sources have been realized as an alternative energy sources in the production of electric power systems in the world [12] and especially in the rural and off-grid areas. Their use is restricted by their variability of these resources due to location, time of the day as well as season of the year and this reduce their reliability [11]. To overcome these restrictions, the solution to adopt for rural areas and remote locations with the use as a combination energy system with several renewable energy sources, such as a wind and solar photovoltaic as hybrid power system that allows off-setting the intermittent nature of these renewable energy sources [11]. In these energy supply systems, their cost-effectiveness is reached on the condition of gaining a high penetration rate and this is possible only by using energy storage systems to transfer the additional energy during off-peak hours to the peak hours [13]. In this research, a new and innovative energy storage system of compressed air energy storage (CAES) have been studied, whose operation is to use the available electric power during low-demand hours to compress air with a compressor and store it in a small reservoir based on the principles of thermodynamics, heat/work conversion, and generate electric power during the high demand hours. In this case the compressed air is heated in a combustion chamber before being released into a pneumatic motor [14] to run the small gas turbine. With this energy storage system, the focus is on the voltage and frequency regulation of wind-solar photovoltaic hybrid power system using a compressed air energy storage system (CAES) [15]. Based on modeling and the dynamic performance of a compressed air energy storage there is an excess energy available in the wind-solar photovoltaic hybrid power system during the low demand that is stored as a compressed air using a compressor. This stored energy is then released during the high demand of loading [16] and used to generate electric power when required.

The general significant process in wind-solar photovoltaic hybrid power systems is to generate electric power based on regular and irregular conditions since any fault in the system leads to the loss of the system's stability condition [11]. Therefore, a wind-solar photovoltaic hybrid needs to generate power based on the current situation to maintain the system's stability [11]. The advantage of

a Compressed Air Energy Storage (CAES) technology is that it balances fluctuations in power generation and power consumption [17] and hence creates a stable power supply system.

During the implementation of the system under variable load condition, the load tracking problem arises, which causes the voltage and frequency instabilities [9]. This means that the frequency deviates from its traditional value whenever there is instability between active power generation and active power load demand [8]. Based on the results, the system should be able to keep the frequency in an acceptable operating range and ensure power quality as required of the system [8]. In the final remark, it was noted that the wind and solar photovoltaic hybrid energy system should operate to provide a stable frequency and voltage for arbitrarily varying loads [13] and an airflow controller should be designed to control the airflow from CEAS to keep the voltage and frequency in an acceptable range [17]. As, compared to other types of energy storage systems such as pumped water, battery, hydrogen and capacitors for energy storage, compressed Air Energy Storage (CAES) is known to be an affordable technology to use in many energy storage applications [15]. During the off-peak period, the CAES system stores the air into an underground reservoir by powering the motor connected to a compressor and during peak periods, the compressed air is utilized to generate power with the turbine [16].

The main novelties and contributions of this research are as follows:

- The development of a micro-grid frequency regulation and enhance the frequency stability against load unbalances in a micro-grid system, a wind and solar hybrid energy containing CAES is proposed.
- The frequency of CAES is adaptively controlled using a PID controller that has been developed in response to load changes. The analog input signal of this controller is the CAES' frequency deviation, which are comparable to the current of 4 to 20 mA. The controller outputs are an analog signal with a current range of 4 to 20 mA for CAES as shown in **Figure 1**.

This study develops an accurate causal steady-state input and output model with an emphasis on airside components for a basic CAES configuration. 2.4 kW air compressor and 1.2 kW pneumatic vane air motor experimental pilot are given. The model is then experimentally validated while paying close attention to each component.

2. CAES Descriptions for Wind-Solar Hybrid Energy

2.1. Compressed Air Energy Storage

For compression and expansion, air energy conversion is considered an isothermal process in which the temperature is constant [18]. The energy conversion process of the proposed system involves three main components: an air compressor, energy storage tank and pneumatic motor or air turbine coupled with an electric generator [19]. The energy conversion starts with the air compressor; the excess electrical power from the wind-solar hybrid power system is

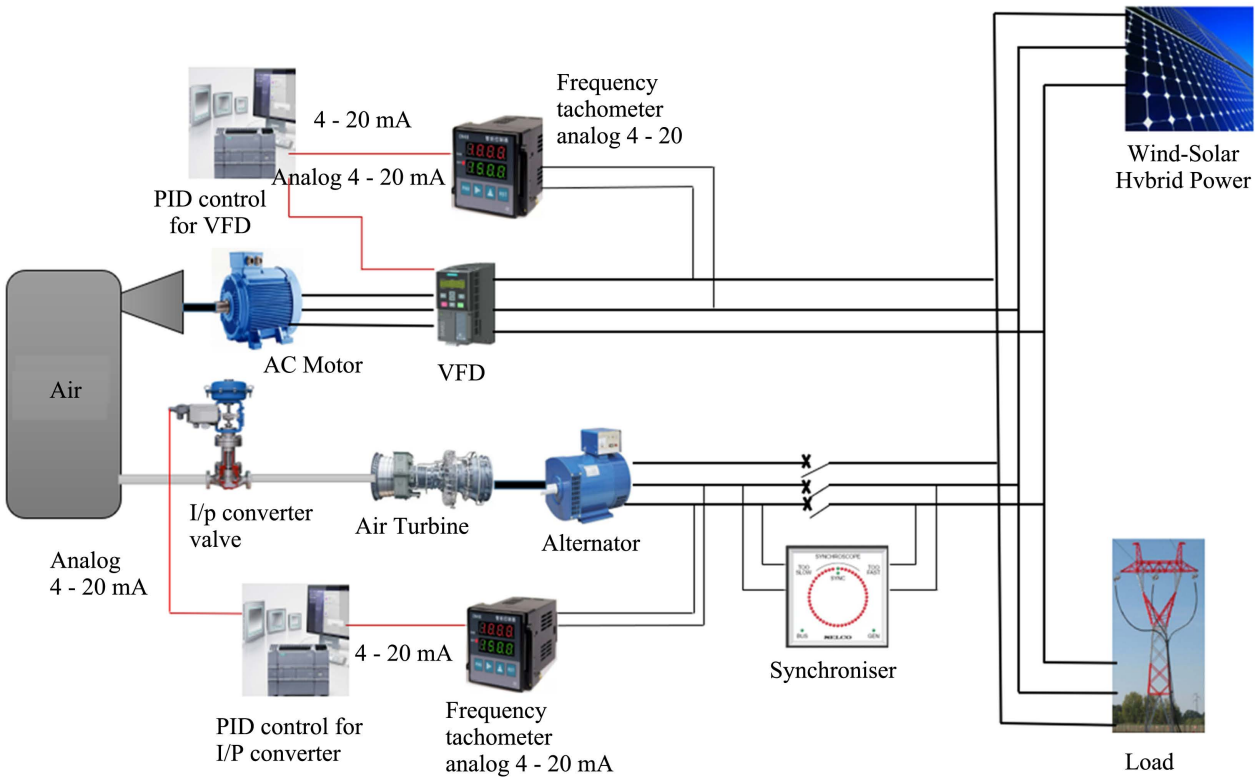

Figure 1. Control system of the CAES during charging and discharging of air into the system, DeKUT Nyeri, Kenya.

converted into mechanical torque for sucking and compressing the air from the atmosphere and storing it in the tank [19]. When power fluctuation occurs in load demand, the compressed air transmits the pressurized air from the air tank to drive the pneumatic motor coupled with an electric generator, which the mechanical power converts back to electric power [15]. Then, compressed air is finally released back into the atmosphere.

With the PID controller in the PLC S7 1200, as applied in this article, the speed of the motor on the air compressor is controlled through VFD, and the airflow through the valve is directed using an I/P converter [20]. So, the power applied to the electric generator is regulated using controlling the speed of the pneumatic motor [15]. During the load application, the voltage and frequency become affected, but voltage and frequency regulation is achieved with the PID controller [15].

2.1.1. Modelling of an Air Compressor

Air compressor is suitable for limited mass flow rate and high-pressure ratio. That why it was most suitable for CAES system design in this work.

An air compressor is used in CAES to increase the air pressure. The compression ratio for each stage is r_c [17];

$$r_c = \frac{P_{\text{out}}}{P_{\text{in}}} \tag{1}$$

where, P_{in} represents inlet pressure, and P_{out} represents outlet pressure.

The efficiency of air compressor η_c is given by [17];

$$\eta_c = 0.91 + \frac{r_c - 1}{300} \tag{2}$$

The outlet temperature of the compressor is T_{out} [17];

$$T_{\text{out}} = T_{\text{in}}\left[1 + \frac{1}{\eta_c}\left(r_c^{\frac{\gamma-1}{\gamma}} - 1\right)\right] \tag{3}$$

where, T_{in} and T_{out} are compressor inlet and outlet temperature, γ is adiabatic index. The power consumption of the compressor is expressed as [15];

$$\dot{W}_c = \frac{1}{\eta_c}\dot{m}C_p T_{\text{in}}\left(r_c^{\frac{\gamma-1}{\gamma}} - 1\right) \tag{4}$$

where, $\dot{W}$ is power output, $\dot{m}$ is mass flow rate of the air. C_p is specific heat capacity of the air.

2.1.2. Modelling of the Pneumatic Motor

A pneumatic motor is used in CAES to expand the air to produce power output. The expansion ratio for each stage is r_p [15];

$$r_p = \frac{P_{\text{in}}}{P_{\text{out}}} \tag{5}$$

where, P_{in} and P_{out} are inlet and outlet pressures respectively. The efficiency η_p of pneumatic motor is expressed as [15]

$$\eta_p = 0.9 - \frac{r_p - 1}{250} \tag{6}$$

The outlet temperature of compressor is $T_{p\text{out}}$ [15]

$$T_{p\text{out}} = T_{p\text{in}}\left[1 - \eta_p\left(1 - r_p^{\frac{1-\gamma}{\gamma}}\right)\right] \tag{7}$$

where, $T_{p\text{in}}$ and $T_{p\text{out}}$ are inlet and outlet temperatures of the pneumatic motor respectively. The power output $\dot{W}_p$ of the pneumatic motor is expressed as [15]

$$\dot{W}_p = \eta_p \dot{m} C_p T_{p\text{in}}\left(1 - r_p^{\frac{1-\gamma}{\gamma}}\right) \tag{8}$$

where, $\dot{W}_p$ is power output, $\dot{m}$ is mass flow rate of the air. C_p is specific heat capacity of the air.

2.2. Variable Speed Wind Turbine

In normal operations, the WT operates at the maximum power point tracking (MPPT) to extract maximum power from the varying wind.

The P_{mppt} is the electric power output of the machine in the MPPT mode that is a cubic function of the rotor speed, ω_r [21]

$$P_{\text{mppt}}(\omega_r) = k_{\text{opt}}\omega_r^3 \tag{9}$$

where k_{opt} is the constant controller gain and coefficient of the MPPT curve. The MPPT operation mode is at the maximum mechanical power extraction, formulated as follows [21]

$$P_m = \frac{1}{2}\rho\pi r^2 C_p(\lambda,\beta)v_w^3 \tag{10}$$

$$C_p(\lambda,\beta) = 0.22\left(\frac{116}{\lambda_i} - 0.4\beta - 5\right)e^{\frac{-12.5}{\lambda_i}} \tag{11}$$

$$\frac{1}{\lambda_i} = \frac{1}{\lambda + 0.08\beta} - \frac{0.035}{\beta^3 + 1} \tag{12}$$

$$\lambda = \frac{r\omega_r}{v_w} \tag{13}$$

where ρ, r, λ, and β are the air density, blade radius, tip-speed ratio and the pitch angle, respectively. The maximum value of mechanical power P_m can be obtained by maximizing the function $C_p(\lambda,\beta)$, which is a nonlinear function of the tip-speed-ratio λ and the blade pitch angle β as formulated in Equations (9)-(13) and illustrated in **Figure 2**. The maximum mechanical power extraction is when the pitch angle $\beta = 0$.

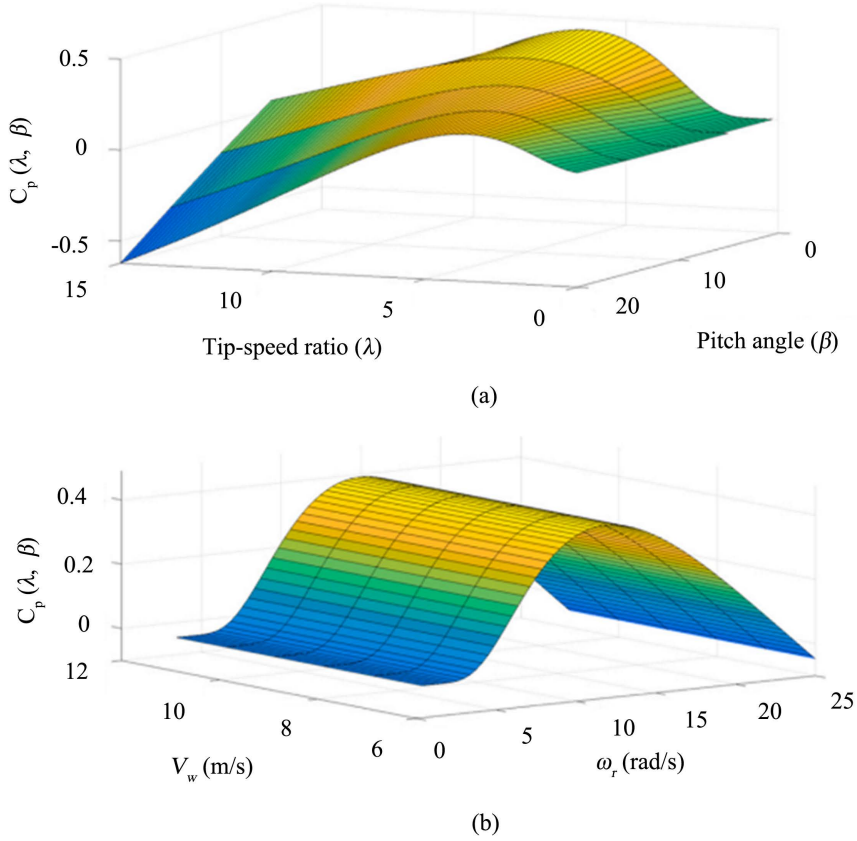

Figure 2. Aerodynamic performance of a wind turbine. (a) as a function of λ_i and β (b) as a function of V_w and ω_r when $\beta = 0$ [9].

2.3. Solar Photovoltaic

The current source I_{ph}, according to [22], represents the cell photocurrent. Taking into account R_{sh} and R_s, which stand for the cell's inherent shunt and series resistances, respectively Since R_{sh} and R_s, typically have very high and low values, respectively, the analysis can be made simpler by ignoring them. Solar PV arrays are made up of parallel-series connections between larger units made up of solar PV cells known as solar PV modules [22]. The following equations can be used to mathematically model a photovoltaic module:

Module photo-current is given by [22]:

$$I_{ph} = \left[I_{SCr} + K_i \left(T - 298 \right) \right] \cdot G/1000 \tag{14}$$

where I_{ph} is the light generated current in a solar PV module (A), I_{SCr} is the solar PV module short-circuit current at 25˚C and 1000 W/m^2, K_i is the short-circuit current temperature co-efficient at I_{SCr} = 0.0017 A/˚C, T is the module operating temperature in Kelvin, G is the solar PV module illumination (W/m^2) = 1000 W/m^2 [23].

Module reverse saturation current, I_{rs}, is given by [22]:

$$I_{rs} = \frac{I_{SCr}}{\left[\exp^{\left(qV_{OC}/N_s kAT \right)} - 1 \right]} \tag{15}$$

where q is electron charge = 1.6 × 10^{-19} C, V_{OC} is the open circuit voltage, N_s is the number of cells connected in series, k is Boltzmann constant = 1.3805 × 10^{-23} J/K, A = B is an ideality factor = 1.6,

The module saturation current I_0 varies with the cell temperature, which is given by:

$$I_0 = I_{rs} \left[\frac{T}{T_r} \right]^3 \exp \left[\frac{q \times E_{go}}{Bk} \left(\frac{1}{T_r} - \frac{1}{T} \right) \right] \tag{16}$$

where T_r is the reference temperature = 298 K, I_0 is the solar PV module saturation current (A), E_{g0} is the band gap for silicon = 1.1 eV [23].

The current output of PV module is:

$$I_{pv} = N_p \times I_{ph} - N_p \times I_0 \times \left[\exp \left[\frac{q\left(V_{pv} + I_{pv} R_s \right)}{N_s AkT} \right] - 1 \right] \tag{17}$$

where N_p is the number of cells connected in parallel, V_{pv} is output voltage of a PV module (V), I_{pv} is output current of a PV module (A), R_s is the series resistance of a PV module. Equations (14)-(17) are used to design the solar photovoltaic model.

2.4. Design of Air Flow Controller

Figure 3 displays the block diagram for the air control system in the CAES. The air flow through the I/P converter valve in this study is controlled by a PID controller. So that, by adjusting the speed of the pneumatic motor, the power applied to the generator is also regulated. During the application of the load, the

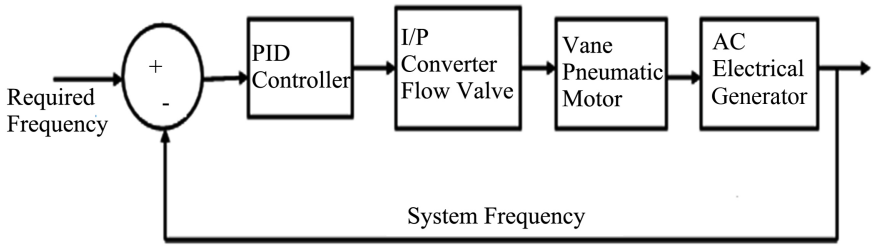

Figure 3. PID control of the airflow in the CAES system.

voltage and frequency get affected. But with PID controller the voltage and frequency stabilities are obtained.

I/P converter converts electrical signals into pneumatic signals by employing the forces in electromagnetic balance theory [24]. I/P converters typically convert 4 - 20 mA of input current into 4 - 120 psi of output [25].

The input current travels through the coil, producing a force that pulls the flapper plate toward it [24]. The nozzle is attracted to current signals more strongly [25]. So, there will also be increased air backpressure. In order to prevent the flapper plate from being affected by shocks or undesired vibrations, the spring balances the flapper plate [24].

An instrument air pressure of at least 120 psi is applied to the flapper valve of the I/P converter [24]. It was calibrated for an output of 4 - 20 mA input is 4 - 120 psi [26]. Most I/P converter may typically be configured to function directly (increasing output pressure as input signal increases). The output signal of an I/P converter quickly reduces to stall pressure in the case of an electrical signal breakdown. This makes it simple to find the device's power failure signal [24].

In several open literatures, the application of a PID controller has been studied [27]. The benefit of a PID controller includes its reliability, simplicity, and independence from the complex mathematical model of a CAES system [28]. Using if-then sets of relationships between the inputs and outputs of the CAES system, PID control methods create the controller based on the expert's understanding of the dynamics of a system [25].

The basic operation of a PID controller is to read a sensor, calculate the proportional, integral, and derivative responses, and then sum these three components to determine the desired actuator output [26]. Before defining a PID controller's settings, it is important to understand what a closed loop system is and some of the terminology used to describe it [24].

For supplementary services, the CAES and wind-solar hybrid energy offer quick dynamic reactions [28]. In this study, the CAES employs a PID controller to respond to voltage and frequency events in an adaptive manner [24]. The voltage and frequency responsiveness of the wind-solar hybrid energy is influenced by the simulated inertial response control [26].

3. Materials and Methods

An overview of the experimental bench work is given at the outset of this section.

The experimental method and operational parameters are then described, followed by a thorough explanation of each component.

Experimental Setup

To design the CAES system suitable for wind-solar hybrid energy, an industrial pilot unit has been built in SIEMENS Laboratory at the DeKUT Nyeri, Kenya. The process instrumentation diagram and photograph are shown in Figure 4 and Figure 5. The related characteristics of each component used to design the CAES system with the loads are described in Table 1.

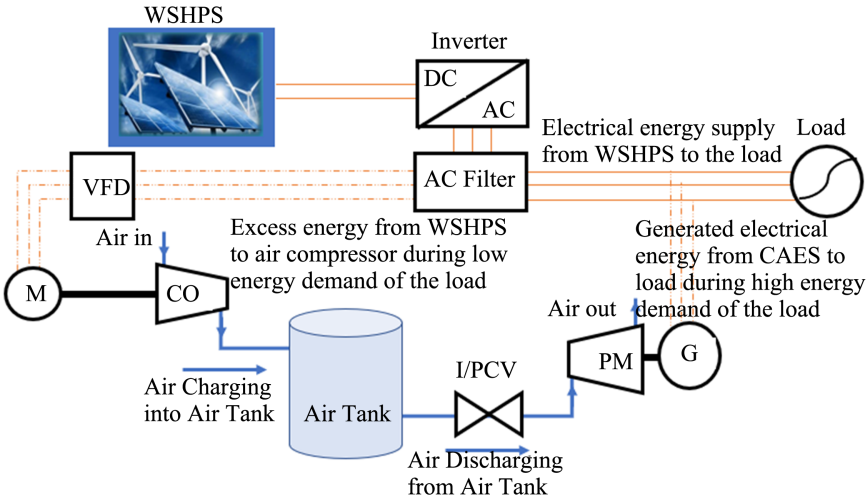

Figure 4. Schematic diagram of a model CAES system. Whereas: WSHPS is wind-solar hybrid power system, VFD is variable frequency drive, G is an electrical generator, I/PCV is an I/P converter valve, PM is a pneumatic motor, CO is an air compressor and M is an electrical motor.

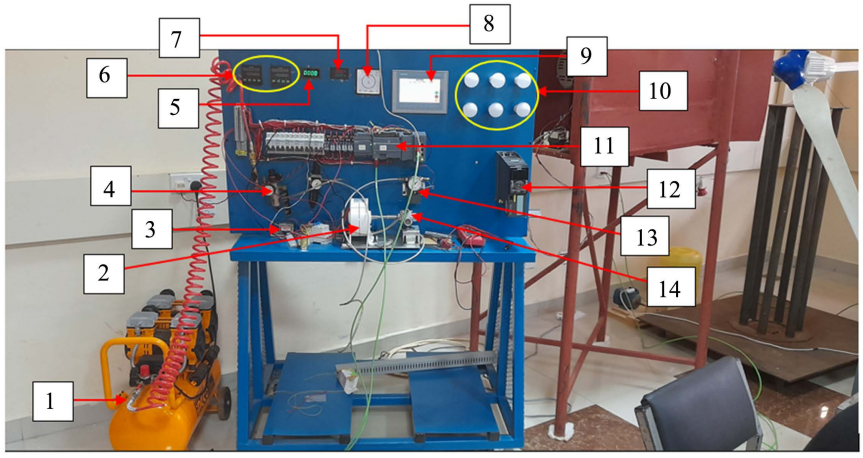

Figure 5. Photograph of the designed CAES system, Siemens Lab_DeKUT, Nyeri, Kenya. 1. Air compressor, 2. AC electrical generator, 3. Step transformer, 4. Air filter, 5. Tachometer RPM speed meter display, 6. IBEST digital frequency meter sensor displays, 7. AC voltage and frequency display, 8. Different energies synchronizer, 9. Human Interface Machine (HMI), 10. Lamps (Loads), 11. S7-1200 siemens PLC, 12. Variable Frequency Drive (VFD), 13. I/P converter valve, and 14. Pneumatic motor.

Table 1. General specification of the CAES system.

1	Air Compressor	Model: ACS224501-8 Power: 3.2 HP Voltage: 220 - 240 V Frequency: 50 Hz Pressure: 8 Bar Air Capacity: 212 L/min@7bar Tank: 50 L
2	Electric Generator	Nominal power = 200 W Line to line Voltage = 24 VAC Frequency = 50 Hz Rotor type → Round Rotor
3	Air Motor	Power = 1.5 hp or 1.2 kW Speed = 3000 RPM Flow rate = 4.7 m^3/min Pressure = 5 Bar
4	I/P converter Valve	422 P/N AC2400 Signal 4 - 20 mA Out 0.2 - 8 bar
5	User/load	30 W

Experimental uncertainties associated with the measurements have been determined from the manufacturer's data as described in Table 1.

The main goal of a CAES is to ensure a continuous supply of the required electrical energy to the load. The initial stage was to design the CAES system that could work in parallel with the wind and solar hybrid power systems. The CAES system design process included the determination of the required parameters of its components, such as the air compressor, air motor, electric generator, and transformer. To fabricate a complete and satisfactory CAES, off-the-shelf components such in GCO Air Compressor, a vane rotary air motor, an electric generator and the transformer were selected according to the capacity of the CAES. The PLC control approach was used to control and protect the CAES by allowing the automatic charging and discharging of the air in the system, hence enabling the CAES to generate the required electricity according to the deficiency to the load.

The surplus of electrical energy from wind and solar hybrid power is therefore stored as pressure potential energy of the compressed air in the air reservoir. When air is extracted from the air reservoir, it is expanded into an air motor which is coupled to an electric generator. The VFD and I/P converter were controlled by a PLC in order to achieve the optimum extraction and expansion of air. Finally, a human machine interface (HMI)/SCADA was assembled to enable

easy monitoring of the functions of CAES.

4. Results and Discussion

4.1. Simulation Results

Simulation results are illustrated in Figures 6-9. The air mass flow rate in the air compressor and the charge and discharge periods of the air into the CAES system during peak and off-peak times are among the characteristics predicted by the simulation results that have been validated by the experimental findings. The maximum inaccuracy is calculated to be 13.1% as follows:

$$\text{error}(\%) = \frac{\text{Simulated result} - \text{Experimental result}}{\text{Maximum}(\text{Simulated result}, \text{Experimental result})}$$

Finally, a detailed analysis for the charge and discharge phases was conducted to study and illustrate the behavior of each component in the CAES system.

The model of the electrical network studied is simulated under the MATLAB/Simulink R2022b environment with a model of the turbine controlled by a PID controller. The appearance of Figure 7, illustrates the elimination of the frequency error by the PID controller after the occurrence of a disturbance.

The PID reacts with the three actions to eliminate the error after approximately two minutes. Figure 8 illustrates the shape of the frequency (in Hz). Frequency deviation is corrected by the PID controller. After a few milliseconds, the measured value approaches the reference value and the action of the derivative makes it possible to obtain frequency stability by a few seconds. This allows the system to participate in primary frequency regulation.

A second simulation is carried out to observe the behavior of the generator after a primary regulation. A disturbance is associated with the system already in a state of disequilibrium with the maximum power of the generator. The controller adjusts the maximum generator output to maintain the frequency shown by Figure 9.

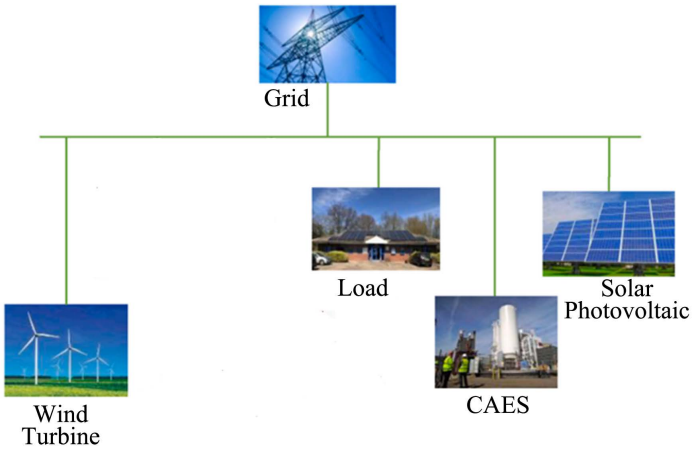

Figure 6. Integrated hybrid renewable energy with CAES and Load in MATLAB/Simulink [7].

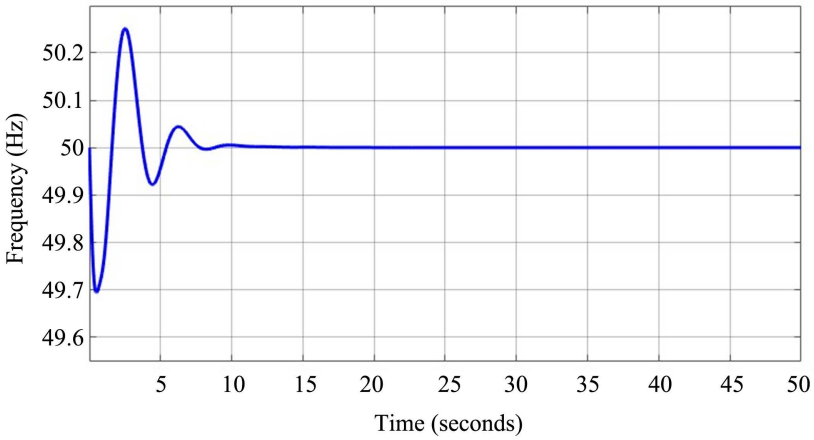

Figure 7. Dynamic system frequency error.

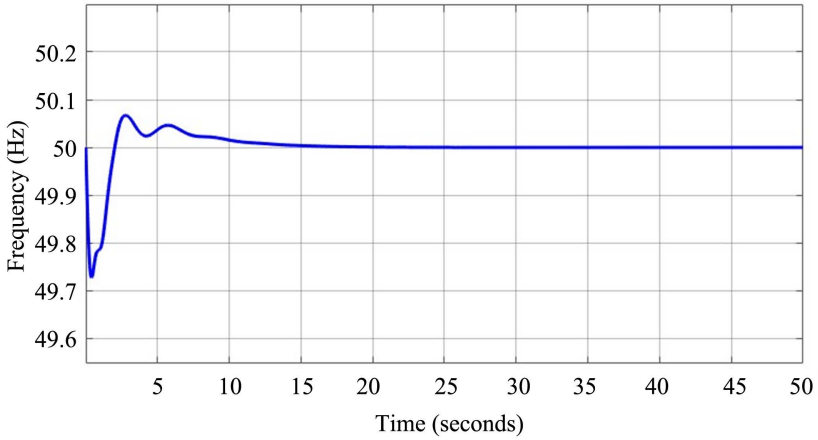

Figure 8. Generator frequency curve for primary regulation.

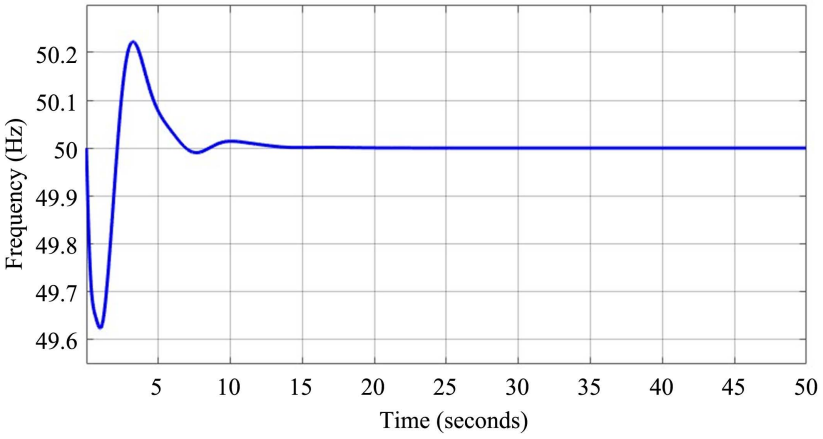

Figure 9. Generator frequency curve for secondary regulation.

4.2. Experimental Results

Experimental results are illustrated in **Figures 10-14.** The practical work consisted in carrying out tests on the power control at suction, then on the pressure control to release the air. An experiment employing a straightforward variable

load was used to validate the established CAES model. An experiment was conducted under various situations, in order to validate the MATLAB/Simulink model. Throughout the experiment, the CAES model was put to the test in a variety of settings. These scenarios included changing the loads while maintaining a constant air pressure, shutting off the loads one at a time while maintaining a constant air pressure, manually adjusting the air pressure to achieve a setpoint frequency under no load, manually adjusting the air pressure to maintain a setpoint frequency while changing the loads, and manually adjusting the air pressure to maintain a setpoint frequency while shutting off the loads one at a time.

Scenarios 1: Changing the loads while maintaining a constant air pressure

In Scenario 1, the loads are periodically turned OFF one by one while keeping the airflow constant. The purpose is to evaluate the sustainability of the power produced by the CAES system. The performance of CAES system is shown in Figures 10(a)-(c). In order to achieve optimal airflow in the I/P converter valve, which receives the instruction from the PID Compact controller programed into PLC S7 1200 using TIA Portal, it is necessary to choose an appropriate setpoint frequency that can serve as a reference point during the regulation of air pressure.

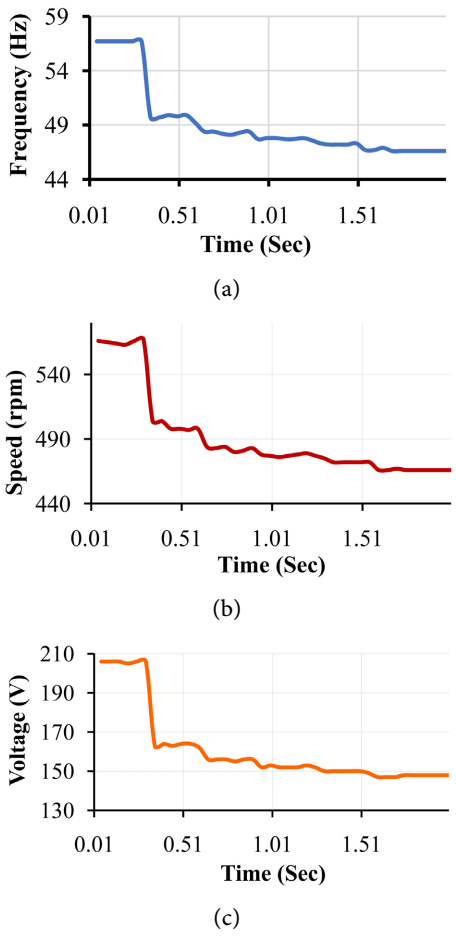

Figure 10. Changing the loads while maintaining a constant air pressure.

An appropriate approach of choosing an airflow controller with a short response time is provided by the identification of a setpoint frequency. Regarding Scenario 3, the PID_Compact controller in TIA Portal is chosen, and its output is confirmed using a PID controller's output in the MATLAB/Simulink environment. The experiments used loads ranging from 5 to 30 W. As shown in Figures 11(a)-(c), off peak is represented by 0 W, and peak is between 5 to 30 W while sustaining airflow by maintaining constant air pressure, the frequency response, rotor speed, and voltage response change from high to low when the loads were changing.

In order to examine how load fluctuations may impact the frequency response, the air pressure is kept constant. Understanding how load variations affect frequency response helps determine a setpoint frequency and the importance of the airflow controller in maintaining a setpoint frequency and ensuring that the loads receive the same frequency throughout the operation. Figures 10(a)-(c) illustrate the performance of the CAES system under load variations. Loads A = 5W, B = 5W, C = 5W, D = 5W and E = 10W, are switched OFF at different time from t = 0.05 sec to t = 1.7 sec. Consider that the power produced by the CAES system does not exceeds the overall load demand. It is evident that, during peak load periods, frequency fluctuates at t = 0.35 sec when load A is instantly added

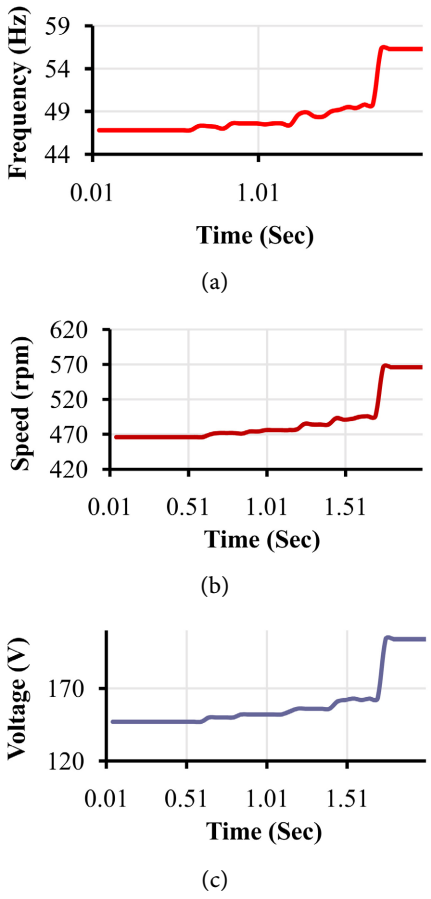

Figure 11. Shutting off the loads one at a time while maintaining a constant air pressure.

consider Figure 10(a), where the air flow was constant due to constant air pressure supply. The frequency continues to fluctuate as load demand increases by adding the loads B, C, D and E at different time. These load variations cause the rotor speed changes as shown in Figure 10(b) which also cause the voltage response to fluctuate Figure 10(c) illustrate. This frequency fluctuation can be successfully reduced by an air flow controller by adjusting the airflow from the CAES system. As how is done at time t = 1.7 sec to time t = 2 sec where the air flow controller regulated the air flow in the system in order to stabilize the frequency response and voltage response by changing the rotor field. The stabilized frequency response, rotor speed, and stabilized voltage response of the CAES system are based on load variations. Voltage fluctuation may be seen at time t = 0.35 sec shown in Figure 10(c) hence the rotor field excitation is changed to instantly suppress it.

Scenarios 2: Shutting off the loads one at a time while maintaining a constant air pressure

In this scenario, the loads are periodically shutting off one by one while maintaining constant airflow. This is done in order to test the capacity and sustainability of the power from CAES system. Figures 11(a)-(c) describe the performance of the proposed CAES system. Scenario 2 also supports the Scenario 1 that there is a need of setting a suitable setpoint frequency that would be a refence during the regulation of air pressure in order to get an optimal airflow in the I/P converter valve which get the command from the PID_Compact controller set into PLC S7 1200. Identification of a setpoint frequency led to a proper selection of controller with a quick response time to the changes. PID_Compact controller in TIA Portal was selected and their result validated it using a result from PID controller in MATLAB/Simulink software as illustrated in Scenario 3. Frequency and Voltage fluctuation under load variations are also shown in Figure 11(a) and Figure 11(c). Loads A = 5W, B = 5W, C = 5W, D = 5W and E = 10W, are switched OFF at different time from t = 0.05 sec to t = 1.7 sec. Suppose that the power produced by the CAES system exceeds the overall load demand. It is evident that, during off-peak load periods, frequency fluctuation starts at t = 0.05 sec as shown in Figure 11(a) caused by high power generation from the CAES system during the off-peak period especially when load A is instantly switched OFF and at where the air flow was constant due to the constant air pressure. The airflow controller worked out this frequency fluctuation by adjusting the airflow from the CAES system by regulating the air pressures leading to change in rotor speed as illustrated in Figure 11(b). During that period, the compressor is turned "OFF." The stabilized frequency response, rotor speed changes, and stabilized voltage response of the CAES system are based on load variations. Voltage fluctuation may be seen at time t = 0.65 sec, Figure 11(c) illustrate, the rotor field excitation is changed to instantly suppress it. The extra electrical power from the microgrid in this instance is turned into mechanical torque and used to draw air from the atmosphere, compress it, and store it in a CAES reservoir.

Scenarios 3: Adjusting the air pressure to achieve a setpoint frequency under off load

The Scenario 3 concern with adjustment the airflow by regulating the air pressures till the setpoint frequency is reached. The setpoint under off peak is set to be 50 Hz as shown in Figure 12(a). The setting took some times to make a clear point of 50 Hz setpoint frequency. The setup was done by setting the setpoint frequency in the PID_Compact controller which is airflow controller in this case using TIA Portal V17 which after was downloaded into PLC S7 1200 to provide an automated control of an I/P converter valve. Then I/P converter valve is used to regulate the air pressures automatically following the order of the setpoint frequency from the PID_Compact controller. The simulation results from MATLAB/Simulink that demonstrate the successful monitoring of the setpoint frequency by merely modifying the controller's parameters are used to validate Scenario 3. The PID_Compact controller was selected for use with the TIA Portal V17 software because it is compatible with the PID controller in the MATLAB/Simulink program. Only the K_P, K_I and K_D parameters of this PID controller can be altered until the desired frequency is attained.

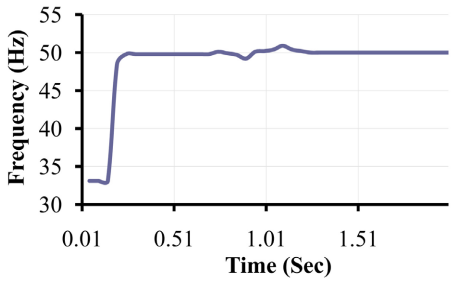

(a)

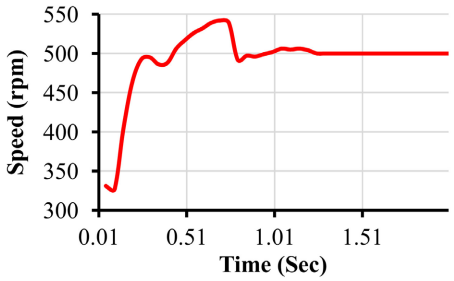

(b)

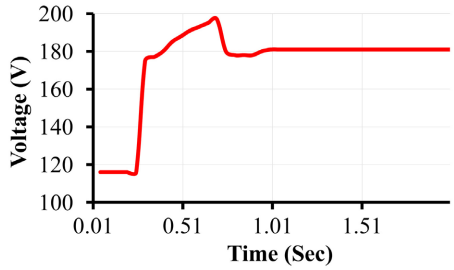

(c)

Figure 12. Adjustment of the air pressure to achieve a setpoint frequency during off peak.

By considering the Figures 12(a)-(c) for the illustration of CAES system for compensating the power deficiency to the load due to load variations. Consider that the entire load power does not be greater than the power generated by CAES system. It is evident that frequency is fluctuating at t = 0.2 sec to t = 1.2 sec caused by high power generation from CAES system during the off-peak period. Then volatility is reduced by using an airflow controller to regulate the airflow. This frequency fluctuation implies that the stored compressed air from the CAES system is used to generate the electrical power when the load power is greater than the microgrid power in order to meet the load requirement.

Figure 12(a), depict the frequency response fluctuation during off peak where it is suppressed effectively by air flow controller by changing air flow from the CAES system leading to the change in rotor speed as shown in Figure 12(b). through this air flow controller, the stabilized frequency response is maintained from t = 1.25 sec, and stabilized voltage response is also maintained from t = 1.05 sec as shown in Figure 12(c) so as to enable the CAES system to respond to the load variations.

Scenarios 4: Regulation of the air pressure to maintain a setpoint frequency while changing the loads

The setpoint frequency of 50 Hz, which it is set under off peak is set, but after switching ON the loads in sequence, the loads power became greater than the power from CAES system, hence the frequency response became lower than the setpoint frequency. Therefore, the new setpoint frequency which can be sustainable during the experiments, was needed to be set. By this point, 46.3 Hz was the selected as setpoint frequency as Figure 13(a) illustrates. All of the loads employed in the trials is to be operating at 46.3 Hz, the only regulation is airflow in order to stabilize the frequency response by controlling the air pressures. The regulation of air pressure was done by airflow controller so to make sure that the setpoint frequency is maintained at 46.3 Hz. This scenario is identical to Scenario 3, which focused on the automatic air pressure adjustment using PID_Compact controller as airflow controller set in PLC S7 1200 with TIA Portal V17 software in response to variations in loads so as to stabilize the frequency response. With MATLAB/Simulink software, Scenario 3 was used to clarify and validate the performance of the airflow controller as shown in Figures 13(a)-(c).

Figures 13(a)-(c) illustrates the performance of the CAES system under load variations. Loads required to be supplied to the CAES system are A = 5W, B = 5W, C = 5W, D = 5W, and E = 10W. These are added in CAES system at different time ranging from t = 0.35 sec to t = 1.55 sec. Consider that the entire load power exceeds the power generated by CAES system. It is evident that frequency is fluctuating at t = 0.6 sec as shown in Figure 13(a) when the load demand starts to be high. The volatility is reduced by using an airflow controller to regulate the airflow by changing the rotor speed as shown in Figure 13(b) and the system's frequency response is stabilized from t = 1.30 sec under load variations. Rotor speed changes can cause the alteration in the rotor field excitation which in turn lead to the stabilized voltage response as shown in Figure 13(c) in the

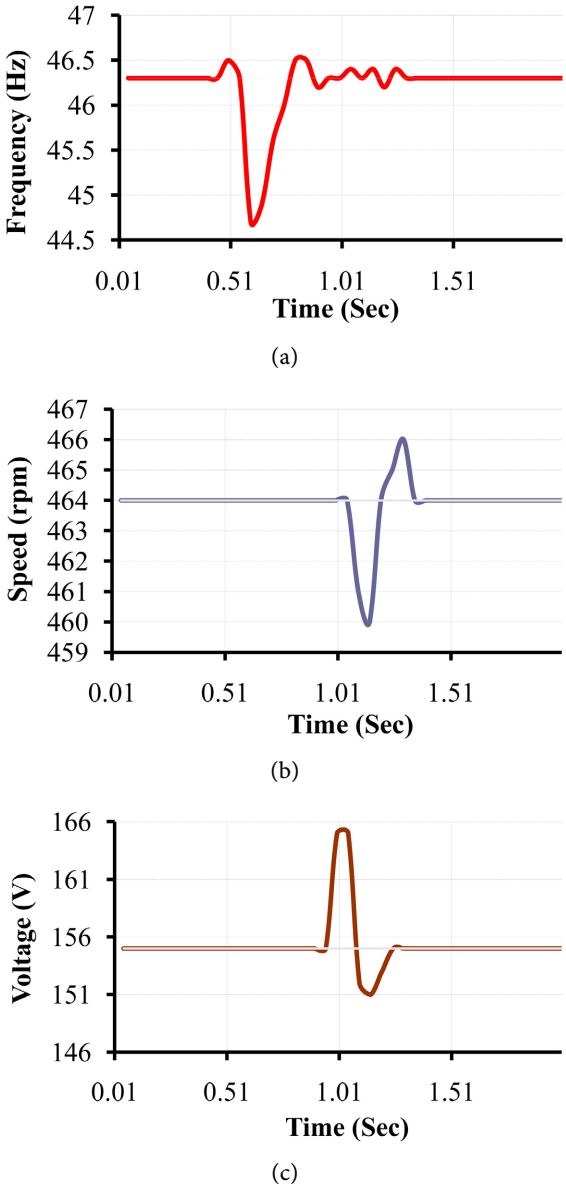

Figure 13. Adjustment of the air pressure to stabilize the setpoint frequency while changing the loads.

CAES system under load variations. The stored compressed air from the CAES system is used to generate the electrical power when the load power is greater than the microgrid power in order to meet the load requirement. In this instance, compressed air is used to convey air power to drive an electric generator coupled to a prime mover, which then turns mechanical power back into electrical power. During this period, the compressor is in "ON" mode throughout that period.

Scenarios 5: Regulation of the air pressure to maintain a setpoint frequency while shutting off the loads one at a time

The veracity of Scenario 4 is supported by Scenario 5. In Scenario 5, the loads were periodically shutting off one by one to test whether the setpoint frequency of 46.3 Hz is sustainable. The frequency obtained up until the point of opera-

tions is 46.5 Hz as Figure 13(a) illustrate with a 0.2 Hz inaccuracy. This frequency variation is too slight to be problematic.

In order to maintain the setpoint frequency of 46.3 Hz while turning off the loads in sequence, the air flow controller is needed to be adjusting the air pressure automatically. The adjustment resulted in an inaccuracy of 0.2 Hz can be caused by machine error or human error making it more challenging to reach the desired setpoint frequency on schedule. And therefore, the air flower controller preferably PID_Compact controller set in the PLC S7 1200 using TIA Portal V17 to monitor the I/P converter, as Scenario 3 validated by simulated results from MATLAB/Simulink software, it is crucial to regulate the I/P converter valve in the experimental setup in order to achieve the ideal air flow to maintain the setpoint frequency stable under fluctuations in load.

As Figures 14(a)-(c) illustrate. Consider loads A, B, C, D, and E as explained in Scenario 4. These loads now are switched OFF at different time from t = 0.05 sec to t = 1.6 sec. Consider that the entire load power does not exceeds the power generated by CAES system. It is evident that frequency is fluctuating at t = 1.2

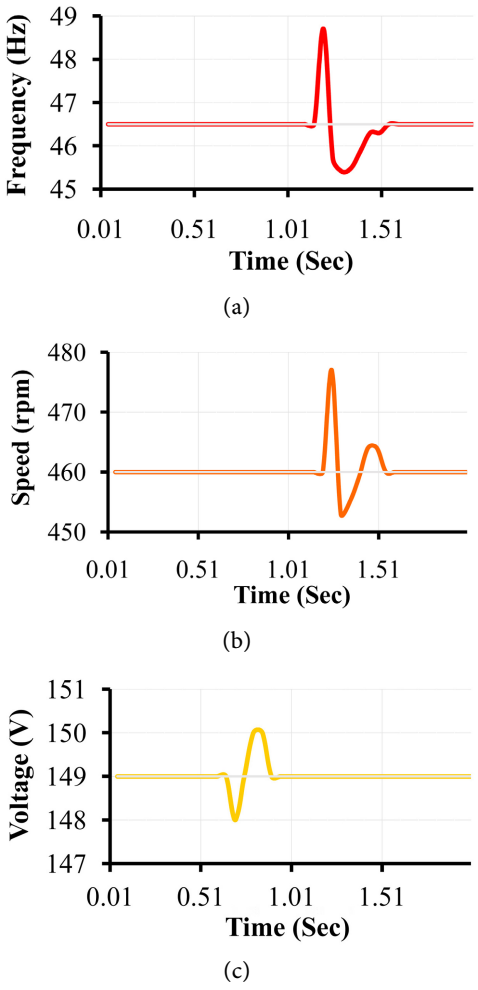

Figure 14. Adjustment of the air pressure to stabilize the setpoint frequency while shutting off the loads one at a time.

sec to 1.4 sec as shown in Figure 14(a) when the load demand starts to be decrease. The volatility is reduced by using an air flow controller to regulate the airflow by changing the rotor speed as shown in Figure 14(b) and the system's frequency response is stabilized from t = 1.45 sec under load variations. Rotor speed changes can cause the alteration in the rotor field excitation which in turn lead to the stabilized voltage response shown in Figure 14(c) in the CAES system under load variations. The stored compressed air from the CAES system is used to generate the electrical power when the load power is greater than the microgrid power in order to meet the load requirement. In this instance, compressed air is used to convey air power to drive an electric generator coupled to a prime mover, which then turns mechanical power back into electrical power. During this period, the compressor is in "OFF" mode throughout that period.

4.3. Results Validation

4.3.1. Response Time

As demonstrated in Figures 7-9, the controller responded to the disturbance in the model simulation in 1 second. However, in the experiments, as shown in Figure 10 and Figure 11, the controller responded to the disturbance in t = 0.35 seconds while the air pressure was kept constant. The controller required t = 0.2 sec to react to the disturbance during air pressure regulation for the experiment shown in Figures 12-14. This response time was necessary to produce the necessary voltage and frequency to the loads.

4.3.2. Stabilization Time

Following the occurrence of the disturbance shown in Figures 7-9, the controller needed one second to stabilize the voltage and frequency to the loads during the model's simulation. As shown in Figure 10 and Figure 11, in the experiment where there was no air pressure regulation, the controller needed t = 1.7 sec to stabilize the voltage and frequency to the loads when the disturbance was applied. Nevertheless, as shown in Figures 12-14, the controller during the experiment with the air pressure regulation required t = 1.25 sec to stabilize the voltage and frequency to the loads following the application of the disturbance.

5. Conclusions

Recently, there has been a sharp rise in the requirement for energy storage, and CAES has a major impact on how this is handled. According to its principles and benefits, CAES is now developing, and this thesis has predicted that it will continue to develop into one of the most promising energy storage technologies. High capacity, high power rating, and long-duration storage are benefits of CAES. The drawbacks of this technology include low power density, substantial transportation losses, and size and geological site restrictions.

This work has detailed a hybrid energy system that includes solar and wind energy with variable speeds, as well as a power electronic interface and CAES system. MATLAB/Simulink was used to carry out computer simulations for hy-

brid energy systems that included solar systems and variable speed wind production. The CAES system's effectiveness is assessed for load variations. AC voltage varies as a result of changes in load. The balance between the source and the load is maintained by the CAES system. The performance of the 12 m/s wind system and the 1000 W/m^2 solar PV system in the hybrid system has been examined. The performance of the control system for the developed prototype of CAES system is validated using the MATLAB/Simulink R2022b simulation, and it has been found that the frequency fluctuation and voltage drop of the developed prototype of CAES system during load variations were governed by the I/P converter using a PID_Compact controller programed in the TIA Portal V17 software and downloaded into PLC S7 1200.

The possible uses of CAES system have been highlighted by this study, including distributed energy and microgrid systems, distributed energy generation, and cogeneration systems. Scientists have a lot of expertise with and a better-defined set of objectives for the mature technology known as CAES system. Furthermore, it showed promised and is anticipated to be combined with other technologies in the future, including solid oxide fuel cells, gas turbines, renewable energy sources, and other systems.

Moreover, based on the review of the current situation, the future research paths of CAES system are anticipated, including further significant increase in efficiency, the need to lower the cost of building air reservoirs, and the investigation of the potential environmental impact.

6. Recommendations

Even though the suggested control system of the CAES system was validated through simulation, there are still a lot of other areas that could use further research and development before this technology is practical for use in the industrial sector. Increasing efficiency and overall energy yields are the main goals of the majority of these domains.

A hardware prototype was also built, along with CAES system monitoring. Owners of CAES system need to be confident that their equipment works well and will be a good investment.

Failures and flaws must be found and corrected right away, regardless of the type of control system that is used, including plant systems, individual systems, and private systems. This could only be accomplished by improving the performance of the system and stopping any degeneration in its tracks.

Conflicts of Interest

The authors declare no conflicts of interest regarding the publication of this paper.

References

[1] Zsiborács, H., *et al.* (2019) Intermittent Renewable Energy Sources: The Role of

Energy Storage in the European Power System of 2040. *Electronics*, **8**, 729. https://doi.org/10.3390/electronics8070729

[2] Khodayar, M.E. (2017) Rural Electrification and Expansion Planning of Off-Grid Microgrids. *The Electricity Journal*, **30**, 68-74. https://doi.org/10.1016/j.tej.2017.04.004

[3] Berardi, U., Tomassoni, E. and Khaled, K. (2020) A Smart Hybrid Energy System Grid for Energy Efficiency in Remote Areas for the Army. *Energies*, **13**, Article No. 2279. https://doi.org/10.3390/en13092279

[4] Misra, S., *et al.* (2021) Integration of Supply and Demand Side Management Using Renewable Power Sources: Application on an Air Separation Plant. *Industrial & Engineering Chemistry Research*, **60**, 3670-3686. https://doi.org/10.1021/acs.iecr.0c05810

[5] Olatomiwa, L., *et al.* (2018) Hybrid Renewable Energy Supply for Rural Healthcare Facilities: An Approach to Quality Healthcare Delivery. *Sustainable Energy Technologies and Assessments*, **30**, 121-138. https://doi.org/10.1016/j.seta.2018.09.007

[6] Østergaard, P.A., *et al.* (2020) Sustainable Development Using Renewable Energy Technology. *Renewable Energy*, **146**, 2430-2437. https://doi.org/10.1016/j.renene.2019.08.094

[7] Hong, Q., Khan, M.A.U., *et al.* (2021) Addressing Frequency Control Challenges in Future Low-Inertia Power Systems: A Great Britain Perspective. *Engineering*, **7**, 1057-1063. https://doi.org/10.1016/j.eng.2021.06.005

[8] Azeem, O., *et al.* (2021) A Comprehensive Review on Integration Challenges, Optimization Techniques and Control Strategies of Hybrid AC/DC Microgrid. *Applied Sciences*, **11**, 6242. https://doi.org/10.3390/app11146242

[9] Du, Y., *et al.* (2020) Damage Detection Techniques for Wind Turbine Blades: A Review. *Mechanical Systems and Signal Processing*, **141**, Article ID: 106445. https://doi.org/10.1016/j.ymssp.2019.106445

[10] Shivashankar, S., *et al.* (2016) Mitigating Methods of Power Fluctuation of Photovoltaic (PV) Sources—A Review. *Renewable and Sustainable Energy Reviews*, **59**, 1170-1184. https://doi.org/10.1016/j.rser.2016.01.059

[11] Kohsri, S., *et al.* (2018) Design and Preliminary Operation of a Hybrid Syngas/Solar PV/Battery Power System for Off-Grid Applications: A Case Study in Thailand. *Chemical Engineering Research and Design*, **131**, 346-361. https://doi.org/10.1016/j.cherd.2018.01.003

[12] Strielkowski, W., *et al.* (2021) Renewable Energy in the Sustainable Development of Electrical Power Sector: A Review. *Energies*, **14**, 8240. https://doi.org/10.3390/en14248240

[13] Samoita, D., *et al.* (2020) Barriers and Solutions for Increasing the Integration of Solar Photovoltaic in Kenya's Electricity Mix. *Energies*, **13**, 5502. https://doi.org/10.3390/en13205502

[14] Borri, E., *et al.* (2022) Compressed Air Energy Storage—An Overview of Research Trends and Gaps through a Bibliometric Analysis. *Energies*, **15**, 7692. https://doi.org/10.3390/en15207692

[15] Mazlan, A.A., *et al.* (2020) Compressed Air Energy Storage System for Wind Energy: A Review. *International Journal of Emerging Trends in Engineering Research*, **8**, 3080-3087. https://doi.org/10.30534/ijeter/2020/34872020

[16] Jin, H., *et al.* (2019) Dynamic Modeling and Design of a Hybrid Compressed Air Energy Storage and Wind Turbine System for Wind Power Fluctuation Reduction.

Computers & Chemical Engineering, **122**, 59-65.
https://doi.org/10.1016/j.compchemeng.2018.05.023

[17] Jakiel, C., *et al.* (2007) Adiabatic Compressed Air Energy Storage Plants for Efficient Peak Load Power Supply from Wind Energy: The European Project AA-CAES. *International Journal of Energy Technology and Policy*, **5**, 296-306.
https://doi.org/10.1504/IJETP.2007.014736

[18] Zhang, X., *et al.* (2018) A Near-Isothermal Expander for Isothermal Compressed Air Energy Storage System. *Applied Energy*, **225**, 955-964.
https://doi.org/10.1016/j.apenergy.2018.04.055

[19] Ibrahim, H., Belmokhtar, K. and Ghandour, M. (2015) Investigation of Usage of Compressed Air Energy Storage for Power Generation System Improving-Application in a Microgrid Integrating Wind Energy. *Energy Procedia*, **73**, 305-316.
https://doi.org/10.1016/j.egypro.2015.07.694

[20] Soe, Y.Y. and San, P.E. (2019) PID Closed-Loop Control Analysis for Automation with Siemens PLC Using TIA V13. *International Journal of Creative and Innovative Research in All Studies*, **2**, 200-208.

[21] Kheshti, M., *et al.* (2022) Liquid Air Energy Storage for Ancillary Services in an Integrated Hybrid Renewable System. *Renewable Energy*, **199**, 298-307.
https://doi.org/10.1016/j.renene.2022.09.010

[22] Bhatia, A. (2008) Design and Sizing of Solar Photovoltaic Systems. (877), 2-125.

[23] Xenophontos, A. and Bazzi, A. (2017) Model-Based Maximum Power Curves of Solar Photovoltaic Panels under Partial Shading Conditions. *IEEE Journal of Photovoltaics*, **8**, 233-238. https://doi.org/10.1109/JPHOTOV.2017.2764488

[24] Yang, H., Wang, W. and Lu, K. (2019) Cavitation and Flow Forces in the Flapper-Nozzle Stage of a Hydraulic Servo-Valve Manipulated by Continuous Minijets. *Advances in Mechanical Engineering*, **11**.
https://doi.org/10.1177/1687814019851436

[25] Newman, H.M. and Morris, M.D. (1994) Direct Digital Control of Building Systems: Theory and Practice. John Wiley & Sons, Hoboken.

[26] Bagyaveereswaran, V., *et al.* (2016) Performance Comparison of Next Generation Controller and MPC in Real Time for a SISO Process with Low Cost DAQ Unit. *Alexandria Engineering Journal*, **55**, 2515-2524.
https://doi.org/10.1016/j.aej.2016.07.028

[27] Ang, K.H., Chong, G. and Li, Y. (2005) PID Control System Analysis, Design, and Technology. *IEEE Transactions on Control Systems Technology*, **13**, 559-576.
https://doi.org/10.1109/TCST.2005.847331

[28] Pivonka, P. (2002) Comparative Analysis of Fuzzy PI/PD/PID Controller Based on Classical PID Controller Approach. 2002 *IEEE World Congress on Computational Intelligence*. 2002 *IEEE International Conference on Fuzzy Systems. FUZZ-IEEE*'02. *Proceedings* (*Cat. No.* 02*CH*37291), Honolulu, 12-17 May 2002, 541-546.